



# PANCHROMATIC STUDY OF STELLAR AND DUST CONTENT OF EARLY TYPE GALAXIES UGC 9519 AND NGC 3699

<sup>1</sup>S. P. Deshmukh & <sup>2</sup>N. D. Vagshette

<sup>1</sup>Department of Physics, Institute of Science, Nagpur -440001,

<sup>2</sup>Department of Physics, Maharashtra Udayagiri College, Udgir, Dist. Latur – 413517,

**Abstract :** • The progress in space technology over past few decades allows researcher to study target galaxies over a wide range of electromagnetic spectrum. In the present study we performed a multi-wavelength analysis of early type lenticular galaxies UGC 9519 and NGC 3699 using optical imaging, spectroscopy, stellar population synthesis and SED fitting. For this study we made use of SDSS data for imaging and spectroscopy. For SED fitting, over a range of UV-Optical- IR region, we used the photometric data by GALEX, SDSS, 2MASS, WISE and IRAS and the MAGPHYS code. The optical colour map of our target galaxies clearly indicates the presence of moderate amount of dust in it. The dust mass is found to be  $4.54 \times 10^5$  and  $7.82 \times 10^7 M_{\odot}$  for UGC 9519 and NGC 3699 respectively. It is observed that, although the present galaxies are of “Red & Dead” class, it holds ongoing star formation activity with the star formation rate equal to  $3.61 \times 10^{-5}$  and  $0.24 M_{\odot}/\text{yr}$  for UGC 9519 and NGC 3699 respectively.

**IndexTerms** – Galaxies, early type galaxies, star formation, interstellar dust, optical spectroscopy, SED fitting.

## I. INTRODUCTION

Early type galaxies usually have the impression of being red and dead galaxies that are composed of the interstellar medium (ISM) and dust. Morphologically, these are featureless bulges. The dominant stellar population in these types of galaxies is the red, evolved, low-mass stars. Due to the lack of dust, these galaxies show a very low level of ongoing star formation compared to the late type galaxies [1,2]. Few early type galaxies may have undergone an active star formation in the past. The energy and radiation coming from these massive stars result in powerful feedback in the form of supernova explosions and strong stellar winds. This feedback drives the available gas out of the galaxy and thus results in the quenching of the star formation activity if any.

Dust provides shielding and cooling off the gas needed for star formation. The lack of dust and the cool gas results in a low level of star formation in early type galaxies. But due to the advent of space technology over the past few decades, it is observed that a considerable sample of early-type galaxies hold multiphase ISM in the form of dust, atomic and molecular gas, ionized gas etc. [3,4]. The origin of this unexpected component in early-type galaxies (ETGs) may be internal or external. The ISM and dust observed in ETGs may arise because of the mass loss by old stellar populations. However, the quantity of ISM component and dust found in samples of ETGs by various methods is found to be higher than expected due to mass loss by old stars. It strongly suggests the external origin of dust and ISM in the ETGs through merger processes or tidal interactions. Indeed, the optical signatures like the presence of dust-lanes, shells, double nuclei, tidal features, etc provide direct evidence of merger-like episodes that took place in the past. Moreover, it could be an AGN or active ongoing, merger-induced star formation that brings these galaxies in the blue cloud region of Color - Mass diagram [5].

To enlighten the origin of dust and ISM in ETGs, it is necessary to observe and analyze many individual early-type galaxies. In this study, we carried out optical imaging, optical spectroscopy, and Spectral Energy Distribution (SED) study of early type galaxies UGC 9519 and NGC 3699.

UGC 9519 is a nearby lenticular galaxy with a redshift of 0.005. It is also named as PGC 052741. Galaxy has been observed by various telescopes and has countable multi-wavelength emission covering UV, IR and radio regions of the electromagnetic spectrum. Galaxy has been observed by IRAS satellite, sensitive to dust emission. It suggests the presence of dust inside the target galaxy. Indeed, the r-band snapshot of UGC 9519 observed by SDSS shows traces of dust in the form of patches lying mainly along the minor axis of the galaxy. Thus UGC9519 may contain low to moderate amounts of dust. This galaxy is observed with the disk inclination with an inclination angle 75 degrees. In this galaxy, there is a very weak or no spiral arm. Its Luminosity Distance is 24.6 Mpc. In UGC 9519, there is no visible central bar. It has no inner or outer stellar ring. No hot spots are visible in the target galaxy. The optical spectrum is found to have H $\alpha$  emission line suggesting the presence of ionized gas in this galaxy. Thus, suggesting certain activity either in the form of AGN and/or star formation in UGC 9519.

NGC 3699 is a nearby edge-on SO-type galaxy with a redshift 0.01. Like UGC 9519, NGC 3699 has countable multi-wavelength emission covering UV, IR and radio regions of the electromagnetic spectrum. The optical image of NGC 3699 suggests the presence of a significant amount of dust in the target galaxy covering about 50% of the surface area of the galaxy. Along with a dust lane, dust is also distributed in the form of multiple patches around. The optical spectrum of the target galaxy is free from the emission lines suggesting no presence of ionized gas in NGC 3699. Global parameters of NGC 3966 are listed in Table 1. Figure 1 shows the SDSS tricolor image of target galaxies.

Throughout the work, we used a flat cosmological model with  $\Omega_M = 0.3$ ,  $\Omega_\Lambda = 0.7$  and  $H_0 = 70 \text{ km s}^{-1}$  and used the initial mass function of [6].



Figure 1: SDSS tricolor image of target galaxies UGC 9519 (left panel) and NGC 3699 (right panel)

## II. DATA COLLECTION AND ANALYSIS

We have made use of multi-wavelength observations of UGC 9519 and NGC 3699 galaxies. The optical imaging and spectroscopic data were acquired from the 7th data release of SDSS in  $u$ ,  $g$ ,  $r$ ,  $i$  and  $z$  pass bands with effective wavelengths of 3543Å, 4770Å, 6231Å, 7625Å, and 9134 Å [7]. The angular resolution of the instrument is about 1.5 arcseconds. In the present study, we have considered the Petrosian magnitudes measurement method [8]. The UV radiation from a galaxy holds much information about the young star hence star formation activity. Further to study the star formation process, we have made use of the Near-UV and Far-UV pass band data from Galaxy Evolution Explorer (GALEX) space mission. These measurements were calibrated to the AB magnitude system of [9] using the GALEX pipeline. The dust absorbs the stellar light and re-emits it in the far infrared this corresponds to dust grain temperature of 20 - 100 K. Apart from this stellar emission from ISM is dominated by near IR radiation. Hence IR data were acquired from different observatory. The near-infrared data of J, H and Ks (Kron magnitudes) passbands of the electromagnetic spectrum were used from Two Micron All Sky Survey (2MASS) Extended Source Catalog (EXC) [10] and for the mid-IR data we have used the Wide-field Infrared Survey (WISE) [11] W1, W2, W3 and W4 pass bands. The Infrared Astronomical Satellite (IRAS; [12]) observational data were used to analysis the far-IR faint source catalog data. For this study SDSS, 2MASS, and WISE observational magnitudes were converted to the AB magnitudes and are corrected for the Galactic dust extinction using [13] reddening maps at  $R_V = 3.1$  using [14] extinction law.

### 2.1 Optical imaging:

For optical imaging and spectroscopy, we have used the Image Reduction and Analysis Facility (IRAF) provided by the National Optical Astronomy Observatory (NOAO). The images obtained from SDSS are preprocessed step-by-step as reported in [2,3,15], such as, bias-subtracted, flat-fielded and image co-addition, further the processed images are cosmic corrected. The background correction was applied by estimating sky background using the box method [16]. Cosmic ray corrected, background subtracted, and exposure corrected images are aligned using *geomap* and *geotran* task. We use *gauss* command to obtain PSF-matched images. In order to know the spacial distribution dust and its extent, we generated  $(g - r)$  colour maps of target galaxies, and are as shown in figure 2.

Table 1: Global parameters for target galaxies UGC 9519 and NGC 3699

Galaxy	UGC 9519	NGC 3966
Object names/ Alternative names	CGCG 192-059 MCG +06-32-097 2MASS J14462112+3422141 SDSS J144621.09 + 342214.0 IRAS 14442 + 3434 PGC 052741	NGC 3986 UGC 06920 CGCG 157-058 2MFGC 09381 SDSSJ115644.08+320118.8
RA; DEC	14:46:21.1; 34:22:14	11:56:44.2 ; 32:01:18
Morphology	S0	So edge-on
B-Magnitude $B_T$	14.0	13.5
$D_{25}$ (Major diameter*Minor diameter)	0.8 x 0.6 arcmin	2.97 x 0.58 arcmin
Redshift(z)	0.005440	0.010884
Luminosity distance	24.6 Mpc	49 Mpc

## 2.2 Optical spectroscopy:

The optical spectrum of a galaxy is an excellent tool to determine the nature of the gas distribution and activity that may be present in the galaxy. Along with it, the optical spectrum is useful to determine the stellar population present in a galaxy. In the present study of the target galaxies UGC 9519 and NGC 3699, the primary data

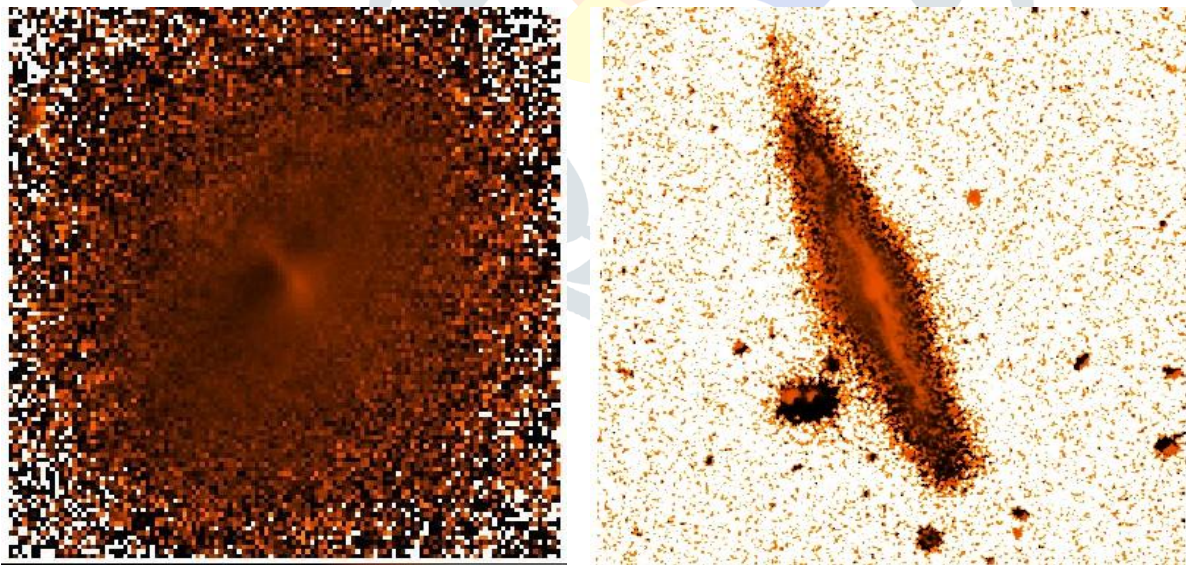


Figure 2: left panel image shows the  $(g - r)$  colour map of UGC 9519 galaxies and the right panel is the colour map of NGC 3966 galaxy.

reduction of SDSS spectrum is done with *onedspec* package in NOAO. The optical spectra of target galaxies were converted into the rest frame spectra using *dopcor* task. Spectra were also corrected for the Galactic extinction using *deredden* task. The stellar population synthesis is performed using STARLIGHT version 04 stellar population synthesis code [17] and REMOVEYOUNG spectral synthesis code of [18]. The linear combination of 45 SSP models was used from [19] this corresponds to a metallicity ( $Z$ ) of 0.2, 1, 2.5 in unit of solar metallicity that comprises fifteen types of stellar age combinations as 0.001, 0.00316, 0.005, 0.01, 0.025, 0.04, 0.102, 0.286, 0.640, 0.905, 1.434, 2.5, 5, 11 and 13 Gyr. STARLIGHT and REMOVEYOUNG fit to the target galaxies are as shown in figure 3. The multiwavelength continuum flux which is free from the nebular emission contribution are used as an input to the REMOVEYOUNG code for further stellar population synthesis. For this study the fraction of stellar population for different ages is as shown in figure 4.

### 2.3 SED fitting:

Fitting of SEDs to the galaxy light over the full range of electromagnetic spectrum is essential to better constrain the properties of a galaxy. A number of codes useful for fitting SEDs of the target galaxies are publicly available and are capable

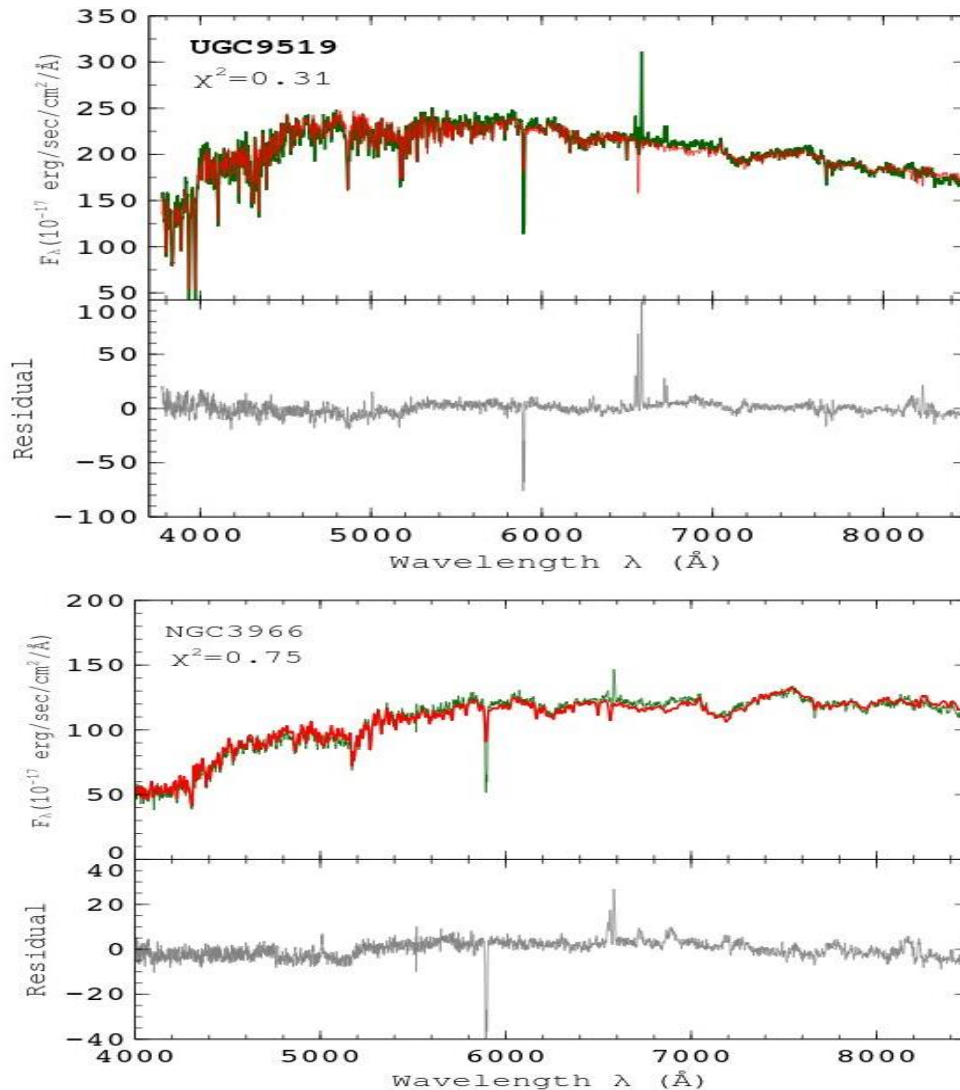


Figure 3: The rest frame optical spectrum of target galaxies fitted with the STARLIGHT code. The green line spectrum is observed spectrum. Red line spectrum is the model fitted by STARLIGHT. Bottom panel in each figure indicates the residual spectrum.

enough to fit the SEDs over the wavelength regime covering UV to Far-IR and even to radio data. For the present galaxies, we used "Multi-wavelength Analysis of Galaxy Physical Properties" (MAGPHYS) [20] code to fit and model the observed SED. MAGPHYS is applicable for low as well as high redshift galaxies with two separate versions built and are widely used by a large range of research community to study various physical properties of galaxies using broad band fluxes. MAGPHYS analyzes the broad-band spectral energy distribution of sample galaxies and gives various physical parameters of the program galaxies as an output.

An empirical but physically motivated SED fitting code MAGPHYS makes use of the optical library of 50000 models with varying star formation histories adopted from 2007 version of [19] stellar population model and IR library of 50,000 models developed by [20] such that each IR model represents an optically thin modified black body emission from different grain sizes, temperature, and emissivity indices. MAGPHYS consider four types of dust components; the Polycyclic Aromatic Hydrocarbons (PAH) molecules, hot dust with temperature range of 130-250 K, warm dust component in thermal equilibrium with temperature range of 30-60K and cool dust with temperature range of 15-25 K. Galactic-disk [6] initial mass function is employed while modeling the stellar emission SED. In order to rule out the effect of attenuation of star light by interstellar dust, a two - component dust model developed by [21] is used. The resultant SED fit to the target galaxies is as shown in figure 3. The quality of the fit was checked from the  $\chi^2$  values. It is an indicator of the goodness of the model fit compared to the data points. The closer the  $\chi^2$  to 1, better will be the fit. The SED fitting for target galaxies is as shown in figure 5. The physical parameters of a galaxy interpreted by MAGPHYS such as stellar mass, dust mass, star formation rate etc are given in table 2.

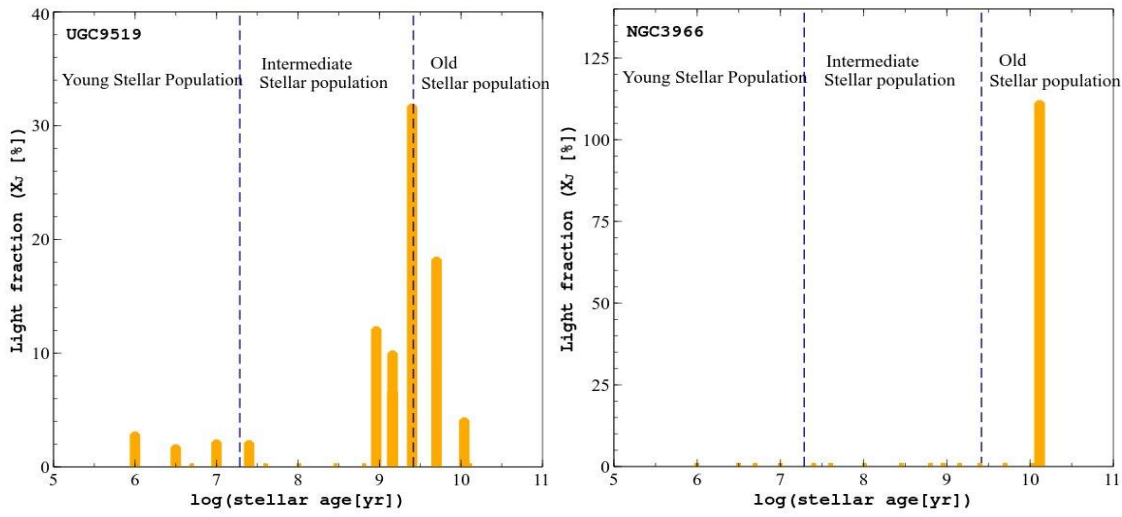


Figure 4: The age wise distribution of stellar population for target galaxies obtained using REMOVEYOUNG code.

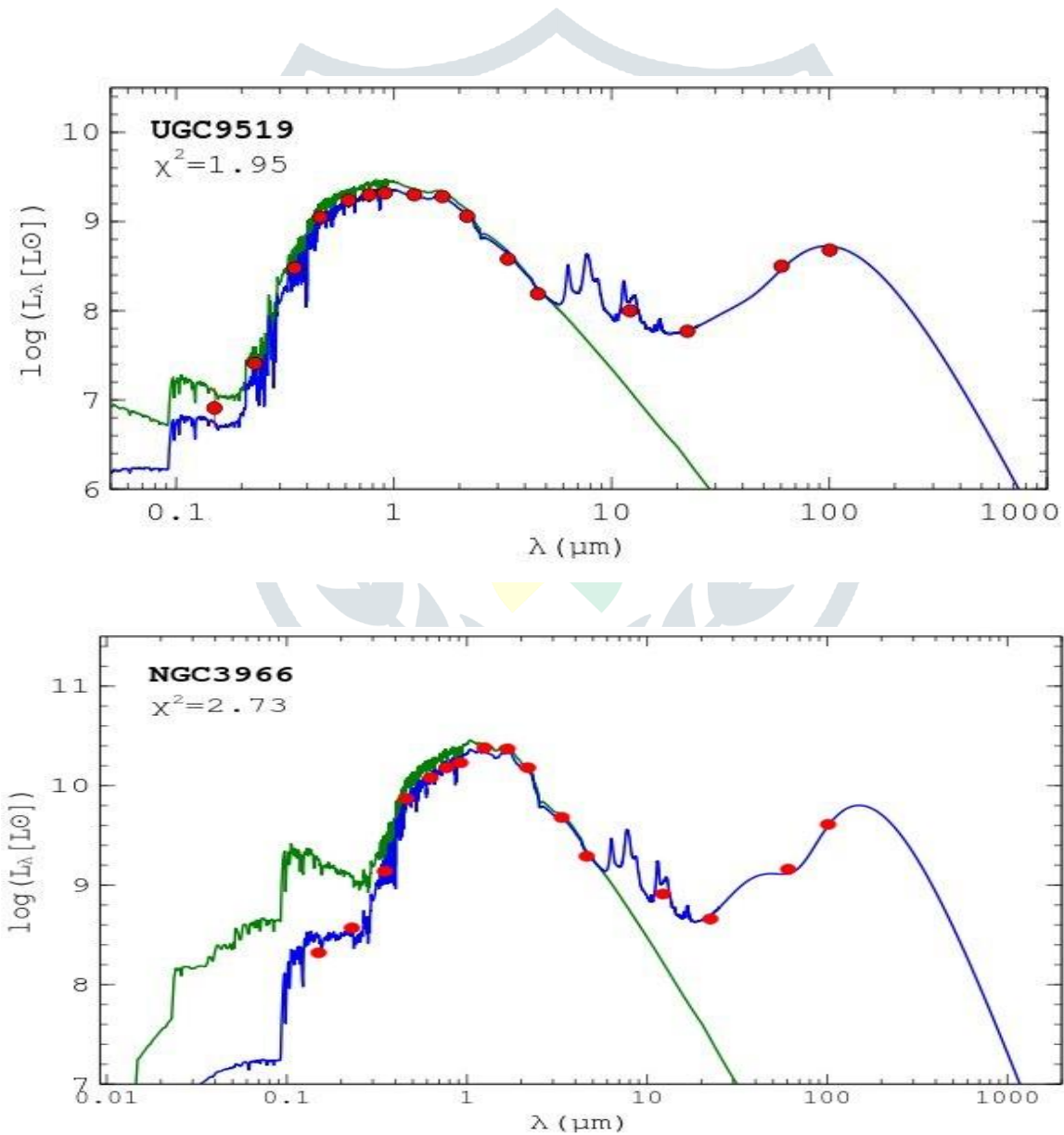


Figure 5:: SED fitting on photometric data of the target galaxies. Attenuated and unattenuated spectra are shown in green and blue color respectively. Red points show photometric data points used for fitting.

Parameters	Description	UGC 9519	NGC 3966
$f_{\mu}$	Fraction of total dust luminosity $L_{dust}$ contributed by the dust in ambient ISM $f_{\mu} = L_{dust}^{ISM} / L_{dust}^{Total}$	0.86	0.8475
$\tau_v$	Total optical depth seen by the young stars in stellar birth cloud	3.17	3.977
$\mu$	Fraction of the $\tau_v$ contributed by the dust in ISM $\mu = \tau_v^{ISM} / (\tau_v^{ISM} + \tau_v^{BC})$	0.101	0.084
$M_{star}$	Stellar mass in $M_{\odot}$	$6.23 \times 10^9 M_{\odot}$	$6.41 \times 10^{10} M_{\odot}$
$L_{dust}^{total}$	Total Luminosity in $L_{\odot}$ absorbed by the dust	$8.124 \times 10^8 L_{\odot}$	$9.238 \times 10^9 L_{\odot}$
$T_c^{ISM}$	Temperature of cold grains in thermal equilibrium in ISM in kelvin	24.5	15.8
$T_w^{BC}$	Temperature of warm grains in thermal equilibrium in birth clouds in kelvin	58.6	57.4
$M_d$	Dust mass in $M_{\odot}$	$4.54 \times 10^5$	$7.82 \times 10^7$
$\Psi$	Star formation rate in $M_{\odot}/yr$	$3.61 \times 10^{-5}$	0.24
$\psi_s$	Specific star formation rate in unit per year, $\psi_s = \Psi / M_{star}$	$5.80 \times 10^{-15}$	$0.386 \times 10^{-11}$

Table 2: The values of physical parameters of the target galaxies interpreted by MAGPHYS

### III. RESULT AND DISCUSSION:

We carried out the multi-wavelength study of ETGs UGC 9519 and NGC 3699 to understand the nature of dust content and stellar content in it. We studied the nature of spectral energy distribution of target galaxies and hence derived various physical parameters. We performed the Stellar Population Synthesis of UGC 9519 and NGC 3699 to understand the age of stellar population in target galaxies.

The (g - r) colour image of target galaxies shows the presence of dust in both galaxies. In UGC 9519, the dust is not well defined, but it shows random distribution that prominently lies along optical minor axis, whereas in NGC 3699, there is well distributed dust that lies along the optical major axis. We have derived dust mass using IRAS colours and is found to be  $2.0179 \times 10^5 M_{\odot}$  and  $5.17 \times 10^6 M_{\odot}$  for UGC 9519 and NGC 3699 respectively. We used the relationships between dust temperature and IRAS flux densities as follows.

$$T_d = 48.93 \times \left( \frac{S(60)_{corrected}}{S(100)_{corrected}} \right)^{0.4}$$

Using IRAS flux densities, dust temperature is found to be 33.89 kelvin and 26.45 kelvin for UGC 9519 and NGC 3699 respectively. Dust mass is calculated using the formula

$$M_d = 4.78 \times S_{100\mu m} \times D^2 \times \left[ \exp\left(\frac{143.88}{T_d}\right) - 1 \right]$$

Where, D is the luminosity distance of the target galaxies obtained from NED. The dust mass predicted by SED fitting for target galaxies UGC 9519 and NGC 3699 is found to be  $4.54 \times 10^5 M_{\odot}$  and  $7.82 \times 10^7 M_{\odot}$  respectively. Thus, the dust content predicted by SED fitting is more than that calculated using IRAS flux densities. This is because, depending on the dust temperature, it emits radiation over a wide range of IR spectrum. Among that range, we have considered only those radiations that fall in the IRAS range.

We studied the nature of spectral energy distribution and hence derived various physical parameters for our target galaxy UGC 9519. Stellar population synthesis of UGC 9519 using SDSS optical spectrum that cover almost 31% galaxy indicates that, although UGC 9519 is an early type galaxy, it carries young as well as moderate age stellar population along with the usual old

stellar population. Although UGC 9519 carries sufficient amount of dust and shows the presence of emission lines in its optical spectrum, the ongoing star formation rate derived by SED fit is found to be very less  $\sim 3.61 \times 10^{-5} M_{\odot}/\text{yr}$ . From SED fitting results, it is clear that the fraction of total dust luminosity  $L_{\text{dust}}$  contributed by the dust in ambient ISM is around 0.8 suggesting that more amount of dust resides in the ambient environment as compared to the stellar birth clouds.

SPS fitting to dusty galaxy NGC 3699 suggests an absence of a young stellar population in it at least in the central region from where the SDSS spectrum is derived. But the SED fit of the target galaxy NGC 3699 suggests a comparatively high star formation rate in it as  $0.24 M_{\odot}/\text{yr}$ . This contradictory result for NGC 3699 may arise because SDSS captures only a small fraction of light, particularly from the center of the galaxy. Whereas the photometric fluxes we have considered for SED fitting include total flux coming from the galaxy. So the result implies that the active star formation in NGC 3699 may span all over the galaxy rather than the central region.

#### IV. CONCLUSION:

This paper presents the optical imaging, spectroscopy, and Spectral Energy Distribution study of nearby early type galaxies UGC 9519 and NGC 3699. We used SDSS DR 7 data for optical imaging and spectroscopy purpose. SED fitting was performed to the UV-Optical-IR data of target galaxies using MAGPHYS code. The main findings of the present study are as follows:

- The optical (g-r) color map of UGC 9519 and NGC 3699 clearly indicates the presence of dust in target galaxies. In UGC 9519, the dust distribution is in the form of patches. In the central region of the target galaxy, dust is found to be lying along optical minor axis. In galaxy NGC 3699, a large amount of dust is observed that lies along optical major axis of the target galaxy and covers larger surface area of the target galaxy. Dust mass, calculated using IRAS flux densities is found to be  $4.54 \times 10^5$  and  $7.82 \times 10^7 M_{\odot}$  for UGC 9519 and NGC 3699 respectively. A more deep observation is required further to know the detailed distribution of dust in these galaxies.
- Contradictory to the nature of being “Red & Dead”, the lenticular galaxies in present study show the signatures of recent star formation activity. SDSS optical spectroscopy and SPS fitting shows that moderate amount of star formation activity is present in GC 9519 and NGC 3699.
- SED fitting of target galaxies estimates various physical parameters of the target galaxy. The star formation rate is found to be  $3.61 \times 10^{-5}$  and  $0.24 M_{\odot}/\text{yr}$  for UGC 9519 and NGC 3699 respectively. Although SDSS spectroscopy doesn't support the presence of young stellar population, the SED fitting of NGC 3699 shows that considerable amount of star formation takes place in it. The contradiction between SED results and SPS results for NGC 3699 is because SDSS aperture is not enough big to cover the whole light coming from the galaxy. It collects light only from the central part of the galaxy. The dust mass calculated by SED fit is found to be  $4.54 \times 10^5$  and  $7.82 \times 10^7 M_{\odot}$  for UGC 9519 and NGC 3699 respectively.

#### IV. ACKNOWLEDGMENT

The present work used the data observed by various observatories. SPD thanks to all the institutes that maintain the data. The SDSS is managed by the Astrophysical Research Consortium for the Participating Institutions. The Participating Institutions are the American Museum of Natural History, Astrophysical Institute Potsdam, University of Basel, University of Cambridge, Case Western Reserve University, University of Chicago, Drexel University, Fermilab, the Japan Participation Group, the Johns Hopkins University, the Joint Institute for Nuclear Astrophysics, the Kavli Institute for Particle Astrophysics and Cosmology, the Korean Scientist Group, the Chinese Academy of Sciences (LAMOST), Los Alamos National Laboratory, the Max Planck Institute for Astronomy (MPIA), the Max Planck Institute for Astrophysics (MPA), New Mexico State University, Ohio State University, University of Pittsburgh, University of Portsmouth, Princeton University, the United States Naval Observatory, and the University of Washington. This work also uses data acquired with the NASA Galaxy Evolution Explorer. GALEX is operated for NASA by the California Institute of Technology under NASA contract NAS5-98034. This publication makes use of data products from the Two Micron All Sky Survey (2MASS). This is a joint project of the University of Massachusetts and the Infrared Processing and Analysis Center/California Institute of Technology, funded by the National Aeronautics and Space Administration and the National Science Foundation. The present work makes use of data products from the Wide-field Infrared Survey Explorer, a joint project of the University of California, Los Angeles, and the Jet Propulsion Laboratory/California Institute of Technology, funded by the National Aeronautics and Space Administration. Some of the data presented in this paper were obtained from the Mikulski Archive for Space Telescopes (MAST). This research has made use of the NASA/IPAC Extragalactic Database (NED) which is operated by the Jet Propulsion Laboratory, California Institute of Technology, under contract with the National Aeronautics and Space administration.

#### REFERENCES

1. Goudfrooij, P., Hansen, L., Jorgensen, H. ~E., and Norgaard-Nielsen, H. ~U. (1994) Interstellar matter in Shapley-Ames elliptical galaxies. II. The distribution of dust and ionized gas. *\aaps*, **105**.
2. Patil, M. ~K., Pandey, S. ~K., Sahu, D. ~K., and Kembhavi, A. (2007) Properties of dust in early-type galaxies. *\aap*, **461**, 103–113.

3. Vagshette, N. ~D., Pandge, M. ~B., Pandey, S. ~K., and Patil, M. ~K. (2012) Dust extinction and X-ray emission from the starburst galaxy NGC 1482. *\na*, **17**, 524–532.
4. Deshmukh, S. ~P., Tate, B. ~T., Vagshette, N. ~D., Pandey, S. ~K., and Patil, M. ~K. (2013) A multiwavelength view of the ISM in the merger remnant galaxy Fornax A. *Res. Astron. Astrophys.*, **13**, 885–898.
5. Faber, S. ~M. (1973) Tidal Origin of Elliptical Galaxies of High Surface Brightness. *\apj*, **179**, 423–426.
6. Chabrier, G. (2003) Galactic Stellar and Substellar Initial Mass Function. *\pasp*, **115**, 763–795.
7. Fukugita, M., Ichikawa, T., Gunn, J. ~E., Doi, M., Shimasaku, K., and Schneider, D. ~P. (1996) The Sloan Digital Sky Survey Photometric System. *\aj*, **111**, 1748.
8. Abazajian, K. ~N., Adelman-McCarthy, J. ~K., Agüeros, M. ~A., Allam, S. ~S., Allende Prieto, C., An, D., Anderson, K. ~S. ~J., Anderson, S. ~F., Annis, J., Bahcall, N. ~A., and et al. (2009) The Seventh Data Release of the Sloan Digital Sky Survey. *\apjs*, **182**, 543–558.
9. Oke, J. ~B., and Gunn, J. ~E. (1983) Secondary standard stars for absolute spectrophotometry. *\apj*, **266**, 713–717.
10. Skrutskie, M. ~F., Cutri, R. ~M., Stiening, R., Weinberg, M. ~D., Schneider, S., Carpenter, J. ~M., Beichman, C., Capps, R., Chester, T., Elias, J., Huchra, J., Liebert, J., Lonsdale, C., Monet, D. ~G., Price, S., Seitzer, P., Jarrett, T., Kirkpatrick, J. ~D., Gizis, J. ~E., Howard, E., Evans, T., Fowler, J., Fullmer, L., Hurt, R., Light, R., Kopan, E. ~L., Marsh, K. ~A., McCallon, H. ~L., Tam, R., Van Dyk, S., and Wheelock, S. (2006) The Two Micron All Sky Survey (2MASS). *\aj*, **131**, 1163–1183.
11. Wright, E. ~L., Eisenhardt, P. ~R. ~M., Mainzer, A. ~K., Ressler, M. ~E., Cutri, R. ~M., Jarrett, T., Kirkpatrick, J. ~D., Padgett, D., McMillan, R. ~S., Skrutskie, M., Stanford, S. ~A., Cohen, M., Walker, R. ~G., Mather, J. ~C., Leisawitz, D., Gautier III, T. ~N., McLean, I., Benford, D., Lonsdale, C. ~J., Blain, A., Mendez, B., Irace, W. ~R., Duval, V., Liu, F., Royer, D., Heinrichsen, I., Howard, J., Shannon, M., Kendall, M., Walsh, A. ~L., Larsen, M., Cardon, J. ~G., Schick, S., Schwalm, M., Abid, M., Fabinsky, B., Naes, L., and Tsai, C.-W. (2010) The Wide-field Infrared Survey Explorer (WISE): Mission Description and Initial On-orbit Performance. *\aj*, **140**, 1868–1881.
12. Neugebauer, G., Habing, H. ~J., van Duinen, R., Aumann, H. ~H., Baud, B., Beichman, C. ~A., Beintema, D. ~A., Boggess, N., Clegg, P. ~E., de Jong, T., Emerson, J. ~P., Gautier, T. ~N., Gillett, F. ~C., Harris, S., Hauser, M. ~G., Houck, J. ~R., Jennings, R. ~E., Low, F. ~J., Marsden, P. ~L., Miley, G., Olmon, F. ~M., Pottasch, S. ~R., Raimond, E., Rowan-Robinson, M., Soifer, B. ~T., Walker, R. ~G., Wesselius, P. ~R., and Young, E. (1984) The Infrared Astronomical Satellite (IRAS) mission. *\ajl*, **278**, L1–L6.
13. Schlegel, D. ~J., Finkbeiner, D. ~P., and Davis, M. (1998) Maps of Dust Infrared Emission for Use in Estimation of Reddening and Cosmic Microwave Background Radiation Foregrounds. *\apj*, **500**, 525–553.
14. Cardelli, J. ~A., Clayton, G. ~C., and Mathis, J. ~S. (1989) The relationship between infrared, optical, and ultraviolet extinction. *\apj*, **345**, 245–256.
15. Deshmukh, S. ~P., Vagshette, N. ~D., and Patil, M. ~K. (2022) Stellar and Dust Properties in a Sample of Blue Early Type Galaxies. *Serbian Astron. J.*, **205**, 23–32.
16. Kulkarni, S., Sahu, D. ~K., Chaware, L., Chakradhari, N. ~K., and Pandey, S. ~K. (2014) Study of dust and ionized gas in early-type galaxies. *\na*, **30**, 51–63.
17. Cid Fernandes, R., Mateus, A., Sodré, L., Stasińska, G., and Gomes, J. ~M. (2005) Semi-empirical analysis of Sloan Digital Sky Survey galaxies - I. Spectral synthesis method. *\mnras*, **358**, 363–378.
18. Gomes, J. ~M., and Papaderos, P. (2016) RemoveYoung: A tool for the removal of the young stellar component in galaxies within an adjustable age cutoff. *\aap*, **594**, A49.
19. Bruzual, G., and Charlot, S. (2003) Stellar population synthesis at the resolution of 2003. *\mnras*, **344**, 1000–1028.
20. da Cunha, E., Charlot, S., and Elbaz, D. (2008) A simple model to interpret the ultraviolet, optical and infrared emission from galaxies. *\mnras*, **388**, 1595–1617.
21. Charlot, S., and Fall, S. ~M. (2000) A Simple Model for the Absorption of Starlight by Dust in Galaxies. *\apj*, **539**, 718–731.